DETERMINATION OF THE BUCKLING LOADS OF IRREGULARLY SHAPED PLATES USING A NEW DESIGN APPROACH

Hesham Ahmed[1], John Durodola[2] and Robert G. Beale[3*]

[1] Ingenieur Buero, Rainfarnstr. 25, 80935 Munich, Germany

[2]Professor，Faculty of Design, Technology and Environment, Oxford Brookes University, Oxford, UK;

[3] Visiting Research Fellow, Faculty of Design, Technology and Environment, Oxford Brookes University, Oxford, UK

* (Corresponding author: Email: rgbeale@brookes.ac.uk)

ABSTRACT

Although elastic buckling has been researched for decades there is still a need to develop fast and comprehensive procedures that will reduce product design time especially during the pre-sizing stage. This paper presents a novel equation and parameters for the buckling analysis of plates that accounts for the interaction of geometry parameters, boundary conditions and different load distributions. The method covers geometrical plate shapes such as triangular, trapezoidal, and slightly curved plates. In the place of classical methods the procedure combines a number of concepts in a novel heuristic manner to achieve a comprehensive solution.

The procedure extends the Euler column buckling boundary condition coefficients to different plate edge boundary condition combinations. Geometry parameters reflect the combined effect of plate aspect ratio and the number of buckle waves. A load parameter introduces a factor that allows the effect of different load distributions to be included in the equation. The method is tested for flat plates of different planar shapes and for slightly curved plates with cylindrical geometries. Eighteen combinations of free, simple support and clamped edge boundary conditions are considered together with uniform and linearly varying edge stress loading conditions. The results are compared with analytical and finite element analyses.

1. Introduction

Following the pioneering work by Bryan [1] in 1890 who determined the buckling load of simply supported rectangular plates, research into two-dimensional plated structures has been carried out by many people and is summarised in standard textbooks such as Timoshenko and Gere [2], Bleich [3], Gerard and Becker [4], Gerard [5] and Bulson [6]. Modern design and analysis of these structures either requires use of the textbooks, such as those in references [2-6] or the use of finite element procedures which require different models when plates of different aspect ratios are analysed or advanced numerical modelling procedures [7-10]. In 2008, Bradford and Roufegarinejad [11] analysed fully clamped rectangular plates under linearly varying axial edge compression. They showed that small variations in the models used for buckling analyses from different investigators for square plates in pure compression gave rise to predictions of the buckling loads varying by up to 30% (in most cases less than 5%). In particular, a model by Liew and Wang [12] using the Rayleigh-Ritz method gave a prediction which was 30% different to the exact solution. The authors in 2013 [14] presented a simple design method to obtain the buckling loads of rectangular plates under a variety of boundary conditions, the results in most cases being within 5% of the exact values. The objective of this paper is to extend the procedure from rectangular plates to planar triangular and trapezoidal plates and to cylindrical rectangular plates. Full details can be found in [15]. Fig. 1 shows the plates considered. The results of the design procedure are compared with those found by the use of MSC/NASTRAN [15] and the German HSB Design Manual [16].
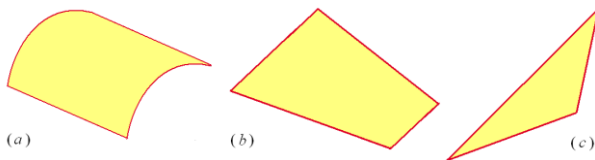

Fig. 1 Irregular plates (a) cylindrical, (b) trapezoidal, (c) triangular

Note that the HSB website [17] states that "The Handbuch Struktur Berechnung [HSB] is a comprehensive reference to procedures, methods, data and tools for the demonstration of sufficient structural integrity of aerospace structures. The manual contains numerous tables, charts, illustrations, and virtually every equation an aerospace design and stress engineer needs. The contents of the manual are updated continuously. The HSB is published by the members of the LTH IASB working group (industry committee for structural analysis documents)."

2. The design procedure for a rectangular plate

The kernel of the procedure is Eq. 1 where the plate buckling equation is given by Eq.1:

$$\sigma_{cr} = [\sigma_{rel}][\beta][\lambda][\eta] \tag{1}$$

where σ_{cr} is the critical buckling stress, σ_{rel} is a plate relative buckling stress parameter; λ is the applied load shape parameter; β is the plate edge support configuration parameter and η is the plate geometry parameter. A schematic of the scope of the methodology is shown in Fig. 2. Note that λ, β and η are dimensionless whereas σ_{rel} has the dimensions of stress (N/mm²).
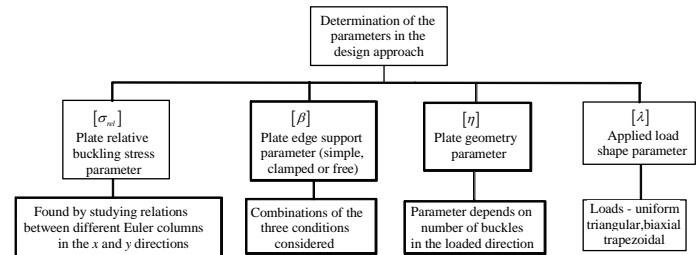

Fig. 2 A schematic of the design methodology

The σ_{rel} term comprises of two terms, $\sigma_{rel,x}$ and $\sigma_{rel,y}$ where these are defined by Eq. 2 and Eq. 3:

$$\sigma_{rel,x} = \left(\frac{\pi}{bt}\right)^2 \left(\frac{EI_y}{a^2}\right) \tag{2}$$

$$\sigma_{rel,y} = \left(\frac{\pi}{at}\right)^2 \left(\frac{EI_x}{b^2}\right) \tag{3}$$

where a and b are the dimensions of a rectangular plate; E, Young's Modulus of Elasticity; t, its thickness; I_x and I_y are the second moments of area of the plate about axes through the centroid of the plate. In determining the plate edge support parameter, β, the four edges of a plate are numbered as shown in Fig. 3 and using the edge boundary combinations shown in Fig. 4 to give the values of β_x and β_y listed in Table 1. Here 's' denotes a simply supported edge, 'c' a clamped edge and 'f' an unsupported or 'free' edge.
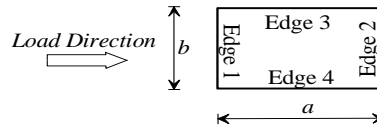
Fig. 3 Edge orientation

Fig. 4 Edge support combinations

Table 1
Values of the edge boundary parameters β_x and β_y for all the plate cases 01 to 18

Case	01	02	03	04	05	06	07	08	09
Edge	ssss	cccc	scsc	ccss	sssc	csss	sscc	sccc	ccsc
β_x	1.000	3.007	1.696	3.007	1.000	1.696	1.000	1.696	3.009
β_y	1.000	1.738	1.369	1.000	1.369	1.000	1.738	1.738	1.369
Case	10	11	12	13	14	15	16	17	18
Edge	ssff	ccff	scff	csfs	ccfc	ccfs	scfc	ssfc	ssfs
β_x	0.763	2.770	1.459	1.496	2.876	2.807	1.565	0.869	0.800
β_y	0.000	0.000	0.000	0.119	0.250	0.119	0.250	0.250	0.119

Table 2
Values of the geometry parameters η_x and η_y

α	0.300	0.375	0.500	0.625	0.750	0.875	1.000	1.125	1.250	1.375	1.500	1.625	1.750	1.875	2.000
ηx	1.271	1.364	1.526	1.715	1.887	2.058	2.198	2.332	2.443	2.555	2.453	2.290	2.155	2.040	1.954
ηy	0.381	0.512	0.763	1.072	1.415	1.800	2.198	2.624	3.054	3.513	3.679	3.721	3.771	3.825	3.907

The aspect ratio is defined to be $\alpha = a/b$. The plate geometry parameter η relates the relative stress, σ_{rel}, to the plate dimensions, i.e. length a and width b. The parameter η has two components or terms, η_x in the plate x-direction, and η_y in the plate y-direction.

The values of η_x and η_y are given in Table 2 and their derivation is given in references [13] and [14]. The coefficients were derived so that the design procedure produces the exact values for the buckling coefficients of a plate simply supported on all four sides [2]. Note that above an aspect ratio of 2.0, that for design purposes, the buckling coefficient can be considered as a constant.

The load distribution parameter λ is used to extend the procedure from uniform axial loading into triangular and trapezoidal loading. Fig. 5 shows triangular loading and Fig. 6 trapezoidal loading where $\sigma_1 > \sigma_2 > 0$.
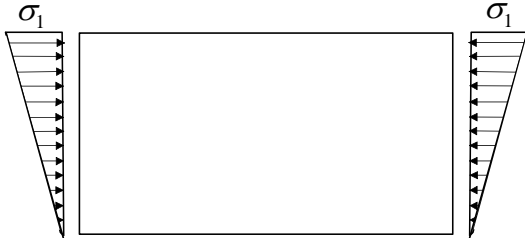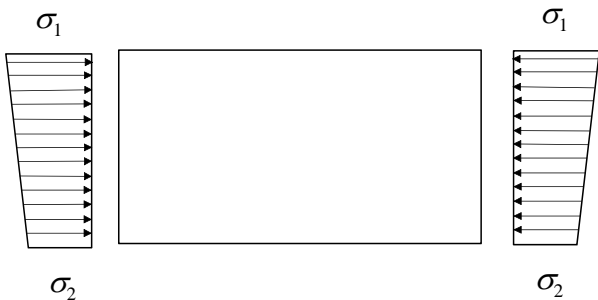

Fig. 5 Triangular loading

Fig. 6 Trapezoidal loading

The load distribution parameter λ was developed in [13, 14] for triangular, trapezoidal and biaxial distributions. The load distribution for triangular loads is given by λ_{tri} for different stress taper forms and boundary conditions in Fig. 7. Note that in Fig. 7 a solid line for an edge implies that the edge is either simply-supported or clamped and a dotted line that the edge is free.

Fig. 7 Values of λ_{tri} for different edge boundary conditions

λ_{trap} for trapezoidal loading is given by Eq. 4:

$$\lambda_{trap} = \left(1 + 0.5\frac{(\sigma_1 - \sigma_2)}{\sigma_1}\right) \tag{4}$$

Before considering plates of triangular, parallelogram or cylindrical shapes let us consider three examples:

2.1. Illustrative example 1

Determine the buckling load of a rectangular aluminium plate with uniform stress applied having a thickness $t = 2.5$ mm, length $a = 90$ mm, width $b = 120$ mm, Young's Modulus of Elasticity $E = 70000$ N/mm^2 and Poisson's ratio $\nu = 0.3$. The plate is fixed in the loading direction and simply-supported in the transverse direction.

Based on the data, $\alpha = 90/120 = 0.75$; $I_y = bt^3/12 = 120 \times 2.5^3/12 = 156.25$ mm^4 and $I_x = at^3/12 = 90 \times 2.5^3/12 = 117.19$ mm^4, then using Eq. 2 and Eq. 3 we obtain

$\sigma_{rel,x} = 44.423$ N/mm^2, and $\sigma_{rel,y} = 24.988$ N/mm^2.

From Eq. 4, for a uniformly distributed load where $\sigma_1 = \sigma_2$ then $\lambda=1.0$.
From Table 1 and for Case 04 we have $\beta_x = 3.007$ and $\beta_y = 1.000$.
From Table 2 $\eta_x = 1.887$ and $\eta_y = 1.415$. Finally substituting into Eq. 5 which is the expanded form of Eq. 1.

$$[\sigma_{cr}] = [\sigma_{rel}][\beta][\lambda][\eta] = (\sigma_{rel,x}\beta_x\lambda_x + \sigma_{rel,y}\beta_y\lambda y) \tag{5}$$

gives $\sigma_{cr} = 287.43$ N/mm^2.

Buckling loads are usually compared with a reference stress, σ_{ref} given by Eq. 6 (which is the Euler buckling load for a rectangular plate simply-supported on all 4 sides):

$$\sigma_{ref} = \frac{\pi^2 E}{12(1-v^2)}\left(\frac{t}{b}\right)^2 \tag{6}$$

where v is Poisson's ratio. For this example, $\sigma_{ref} = 27.46$ N/mm^2. The buckling load factor, k, in this case is $k, = 287.42/27.46 = 10.47$. This compares with values from a Finite Element Analysis using MSC Nastran [15] of 9.36 and DLUBAL [18] of 9.35.

Fig.8 shows the buckling coefficients (k) for the complete range of aspect ratios together with comparisons with FE calculations. The abbreviation for the new design procedure used in Fig. 8 and others is PBA (Parametric Buckling Analysis).
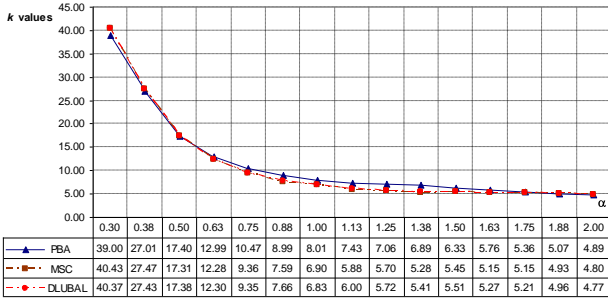
	0.30	0.38	0.50	0.63	0.75	0.88	1.00	1.13	1.25	1.38	1.50	1.63	1.75	1.88	2.00
PBA	39.00	27.01	17.40	12.99	10.47	8.99	8.01	7.43	7.06	6.89	6.33	5.76	5.36	5.07	4.89
MSC	40.43	27.47	17.31	12.28	9.36	7.59	6.90	5.88	5.70	5.28	5.45	5.15	5.15	4.93	4.80
DLUBAL	40.37	27.43	17.38	12.30	9.35	7.66	6.83	6.00	5.72	5.41	5.51	5.27	5.21	4.96	4.77

Fig. 8 *k*-values for a plate with clamped edges loaded and side edges simply-supported

2.2. Illustrative example of a plate subjected to triangular loading

Determine the buckling load factor of a rectangular steel plate with a triangular stress applied having a thickness $t = 5.0$ mm, length $a = 2000$ mm, width $b = 1500$ mm, Young's Modulus of Elasticity $E = 210$ kN/mm^2 and Poisson's ratio $v = 0.3$. The plate is simply-supported on three sides and fixed on the loading edge.

As before $\alpha = 2000/1500 = 1.333$.
Hence, using Eq. 2 and Eq. 3 $\sigma_{rel,x} = 1.0795$ N/mm^2 and $\sigma_{rel,y} = 1.9191$ N/mm^2.
From Table 1 and for Case 06 we have $\beta_x = 1.696$ and $\beta_y = 1.000$.
From Table 2, $\eta_x = 2.518$ and $\eta_y = 3.360$ (using linear interpolation for an aspect ratio between two of the tabulated values).
From Table 3 $\lambda_{tri} = 1.67$.
Substituting into Eq. 1 and treating the terms as vectors

$$[\sigma_{cr}] = [\sigma_{rel}][\lambda][\eta] = (\sigma_{rel,x}\beta_x\lambda_{tri}\eta_x + \sigma_{rel,y}\beta_y\lambda_{tri}\eta_y) \tag{7}$$
$$= (1.0795\times1.696\times1.67\times2.518 + 1.9191\times1.000\times1.67\times3.36) = 18.466 \text{ N/mm}^2$$

As given in example 1, buckling loads are usually compared with the reference stress, given in Eq. 6:

$$\sigma_{ref} = \frac{\pi^2 210000}{12(1-0.3^2)}\left(\frac{5}{1500}\right)^2 = 2.109 \text{ N/mm}^2$$

Hence, the buckling load factor, k, in this case is $k = 18.466/2.109 = 8.76$. This compares with values from a Finite Element Analysis using MSC Nastran [15] of 8.29 and DLUBAL [18] of 8.33. Fig. 9 gives the buckling load factors for the complete range of aspect ratios for this load case with comparisons against finite element calculations.

$$[\sigma_{cr}] = [\sigma_{rel}][\beta][\lambda][\eta] = (\sigma_{rel,x}\beta_x\lambda_{trap}\eta_x + \sigma_{rel,y}\beta_y\lambda_{trap}\eta_y)$$
$$= (1.2282\times1.000\times1.375\times2.453 + 2.7635\times1.000\times1.375\times3.679) \tag{9}$$
$$= 18.122 \text{ N/mm}^2$$

The reference stress, σ is given in Eq. 6:

$$\sigma_{ref} = \frac{\pi^2 210000}{12(1-0.3^2)}\left(\frac{4}{1000}\right)^2 = 3.037 \text{ N/mm}^2$$

Hence, the buckling load factor, k, in this case is $k = 18.1225/3.037 = 5.97$. This compares with values from a Finite Element Analyis using MSC Nastran [15] of 5.96 and DLUBAL [18] of 5.92. See Fig. 10 for a range of aspect ratios for buckling under trapezoidal load with $\sigma_2/\sigma_1 = 0.25$

	0.30	0.38	0.50	0.63	0.75	0.88	1.00	1.13	1.25	1.38	1.50	1.63	1.75	1.88	2.00
PBA	33.19	24.33	16.85	12.86	10.76	9.61	9.00	8.69	8.54	8.68	8.26	7.75	7.41	7.28	7.19
MSC	34.38	25.77	17.60	13.67	10.97	9.63	8.87	8.47	8.31	8.27	8.26	8.20	8.08	7.95	7.84
HSB	34.41	25.82	17.66	13.72	11.01	9.66	8.92	8.53	8.35	8.31	8.29	8.25	8.14	8.00	7.87

Fig. 9 Buckling load factors for case 06 under triangular loading

2.3. Illustrative example for a plate subjected to trapezoidal loading

Determine the buckling load factor of a rectangular steel plate with uniform stress applied having a thickness $t = 4.0$ mm, length $a = 1500$ mm, width $b = 1000$ mm, Young's Modulus of Elasticity, $E = 210$ kN/mm^2 and Poisson's ratio $v = 0.3$. The plate is fixed on all sides and the ratio of axial force is $\sigma_1/\sigma_2 = 0.25$.

$\alpha = 1500/1000 = 1.5$; and hence $\sigma_{rel,x} = 1.2282$ N/mm^2, and $\sigma_{rel,y} = 2.7635$ N/mm^2.
From Table 1 and for Case 01 we have $\beta_x = 1.000$ and $\beta_x = 1.000$.
From Table 2, $\eta_x = 2.453$ and $\eta_y = 3.679$.
From Table 3. $_{tri} = 1.67$.
Using Eq. 4:

$$\lambda_{trap} = \left(1 + 0.5\frac{(1.0-0.5)}{1.0}\right) = 1.250 \tag{8}$$

Finally substituting into Eq. 1 and treating the terms as vectors

$$[\sigma_{cr}] = [\sigma_{rel}][\beta][\lambda][\eta] = (\sigma_{rel,x}\beta_x\lambda_{trap}\eta_x + \sigma_{rel,y}\beta_y\lambda_{trap}\eta_y)$$
$$= (1.2282\times1.000\times1.375\times2.453 + 2.7635\times1.000\times1.375\times3.679) \tag{9}$$
$$= 18.122 \text{ N/mm}^2$$

The reference stress, σ_{ref} is given in Eq. 6:

$$\sigma_{ref} = \frac{\pi^2 210000}{12(1-0.3^2)}\left(\frac{4}{1000}\right)^2 = 3.037 \text{ N/mm}^2$$

Hence, the buckling load factor, k, in this case is $k = 18.1225/3.037 = 5.97$. This compares with values from a Finite Element Analysis using MSC Nastran [15] of 5.96 and DLUBAL [18] of 5.92. See Fig. 10 for a range of aspect ratios for buckling under trapezoidal load with $\sigma_1/\sigma_2 = 0.25$.
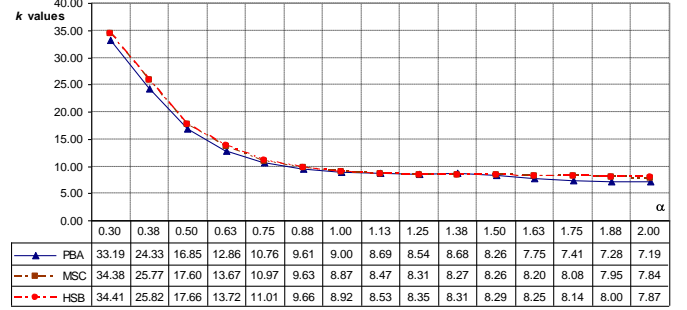
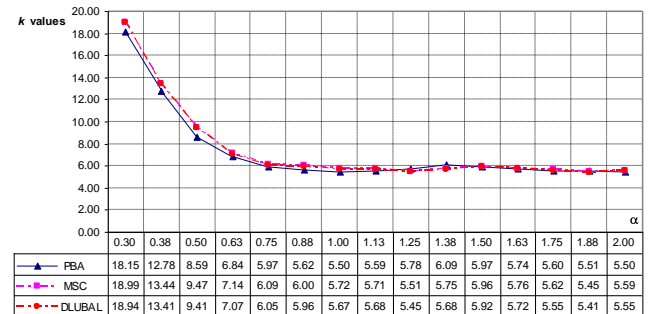|	0.30	0.38	0.50	0.63	0.75	0.88	1.00	1.13	1.25	1.38	1.50	1.63	1.75	1.88	2.00
PBA	18.15	12.78	8.59	6.84	5.97	5.62	5.50	5.59	5.78	6.09	5.97	5.74	5.60	5.51	5.50
MSC	18.99	13.44	9.47	7.14	6.09	6.00	5.72	5.71	5.51	5.75	5.96	5.76	5.62	5.45	5.59
DLUBAL	18.94	13.41	9.41	7.07	6.05	5.96	5.67	5.68	5.45	5.68	5.92	5.72	5.55	5.41	5.55

Fig. 10 Buckling load factors for case 01 under trapezoidal loading for $\sigma_s/\sigma_2 = 0.25$

3. Evolutive plates

Eq. 5 describes only the case of rectangular plates. To extend the geometry based plate stability analysis method to include non-rectangular plates a modification of the plate relative buckling stress parameter σ_{rel} is required. Fig. 11 shows the evolutive plate used in this analysis. The analysis below allows for two different direct stresses, σ_1 acting normal to side length b_1 and σ_2 acting normal to side length b_2. Depending on the choice of σ_1, b_1, σ_2 and b_2 reactive normal and shear stresses may occur on the adjacent to sides of b_1, b_2 stress. The corresponding out of balance forces are supported by boundaries adjacent to b_1, and b_2. The aspect ratios relative to the dimensions of the two ends of the plate, α_1 and α_2, are given by $\alpha_1 = a/b_1$ and $\alpha_2 = a/b_2$ plates a modification of the plate relative buckling stress parameter σ_{rel} is required. Fig. 11 shows the evolutive plate used in this analysis. The analysis below allows for two different direct stresses, σ_1 acting normal to side length b_1 and σ_2 acting normal to side length b_2. Depending on the choice of σ_1, b_1, σ_2 and b_2 reactive normal and shear stresses may occur on the adjacent to sides of b_1, and b_2 stress. The corresponding out of balance forces are supported by boundaries adjacent to b_1, and b_2. The aspect ratios relative to the dimensions of the two ends of the plate, α_1 and α_2, are given by $\alpha_1 = a/b_1$ and $\alpha_2 = a/b_2$.
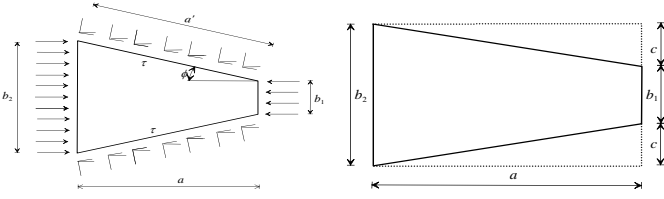

Fig. 11 Evolutive plate

Relating the problem of the evolutive plate to that of the full plate in Fig. 12 by projecting to the left or to the right, it is possible to find a square portion where $a = b_2 = 1$. This gives aspect ratios, $\alpha_1 = 1/b_1$ and $\alpha_2 = 1/b_2$. The change in the longitudinal plate relative buckling stress $\sigma_{rel,x}$ of the plate is related to the change of the aspect ratio from the long edge b_2 to the short edge b_1 of the trapezoidal plate.
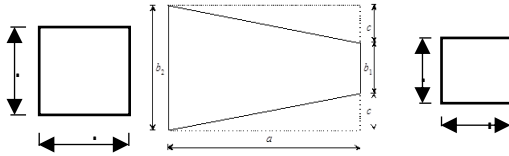

Fig. 12 Evolutive plate and its equivalent rectangular plate

The modification parameter, δ_x is written as:

$$\delta_x = \alpha_1 \cdot \alpha_2 = 1/b_1 \tag{10}$$

The plate's lateral y-direction has width b variable. The lateral plate relative buckling stress parameter δ_y is determined from the plate lateral variation of the evolutive plate.

The area of the evolutive plate in Fig.12 is A_e and the area of the triangles A_t are given in Eq.11 and Eq. 12.

$$A_e = (b_1 + c) \tag{11}$$

$$A_t = ca \tag{12}$$

Converting the evolutive plate in Fig.11 into square plates in Fig. 12 with an aspect ratio α the areas A_e and A_t have edge lengths l_e and l_t which are given in Eq. 13 and Eq. 14 after applying $\alpha = 1.0$ in the plate x - direction and taking the square root of the area.

$$l_e = \sqrt{b_1 + c} \tag{13}$$

$$l_t = \sqrt{c} \tag{14}$$

The lateral plate relative buckling stress parameter δ_y is given in Eq. 15.

$$\delta_y = l_e + l_t = \sqrt{b_1 + c} + \sqrt{c} \tag{15}$$

The values of δ_x and δ_y for the cases $b_1/b_2 = 0.4$, $b_1/b_2 = 0.6$, $b_1/b_2 = 0.8$ and $b_1/b_2 = 1.0$ at the load condition $\sigma_1/\sigma_2 = 1$ are presented in Table 3. Note that σ_1 and σ_2 are the applied stresses along edges b_1 and b_2 respectively.

Table 3
Values of δ_x and δ_y for $\sigma_1/\sigma_2 = 1.0$

σ_1/σ_2	c	b_1/b_2	δ_x	δ_y
	0.30	0.40	$=1.00/0.4$	$=1.00+\sqrt{0.3}$
1.0			$=2.50$	$=1.548$
	0.20	0.600	$=1.00/0.6$	$=1.00+\sqrt{0.2}$
			$=1.67$	$=1.447$
	0.10	0.8	$=1.00/0.8$	$=1.00+\sqrt{0.1}$
			$=1.25$	$=1.316$

Values of δ_x and δ_y for the cases, $_1/b_2 = 0.4$, $b_1/b_2 = 0.6$, $b_1/b_2 = 0.8$ and $b_1/b_2 = 1.0$ are calculated by relating the load condition $\sigma_1/\sigma_2 = 1.0$ to the load conditions $\sigma_1/\sigma_2 = 0.8$ and $\sigma_1/\sigma_2 = 1.2$.

Now, let the parameter relating the stress ratio $\sigma_1/\sigma_2 = 0.8$ to the regular stress ratio $\sigma_1/\sigma_2 = 1.0$ be $\mu_{0.8}$, the parameter relating the stress ratio $\sigma_1/\sigma_2 = 1.2$ to the regular stress ratio $\sigma_1/\sigma_2 = 1.0$ be $\mu_{1.2}$, and the parameter representing $\sigma_1/\sigma_2 = 1.0$ is $\mu_{1.0}$. The increment values for both cases $\mu_{0.8}$ and $\mu_{1.2}$ relative to $\mu_{1.0}$ are given in Eq. 16.

$$\Delta\mu = \pm 0.1\mu_{1.0} \tag{16}$$

The sign for the load condition $\mu_{0.8}$ is positive. This is because the plate is subjected to less loads and consequently the plate critical stress would increase. Whilst, the negative sign is for the load condition $\mu_{1.2}$, because the applied stresses are higher and consequently the plate critical stress will be lower. The values of μ for $\sigma_1/\sigma_2 = 0.8$ and $\sigma_1/\sigma_2 = 1.2$ are calculated from Eq. 17 and Eq. 18, respectively.

$$\mu_{0.8} = (1.0 + 0.1)\mu_{1.0} \tag{17}$$

$$\mu_{1.2} = (1.0 - 0.1)\mu_{1.0} \tag{18}$$

The values of μ for the values of b_1/b_2 and σ_1/σ_2 are put together in Table 4 where the value ± 0.1 is modified according to the value of b_1/b_2.

Table 4
Values of μ

σ_1/σ_2	b_1/b_2	$\Delta\mu$	μ
	0.40	$+0.1 \times 0.4 = +0.4$	1.04
0.8	0.60	$+0.1 \times 0.6 = +0.6$	1.06
	0.80	$+0.1 \times 0.8 = +0.8$	1.08
	1.00	$+0.1 \times 1.0 = +1.0$	1.10
	0.40	$-0.1 \times 0.4 = -0.4$	0.96
	0.60	$-0.1 \times 0.6 = -0.6$	0.94
1.2	0.80	$-0.1 \times 0.8 = -0.8$	0.92
	1.00	$-0.1 \times 1.0 = -1.0$	0.90

The change of the plate relative buckling stress $\sigma_{rel,y}$ in the lateral direction is governed by the lateral change in area of the square and trapezoidal plates, i.e. the plate with trapezoidal edges is converted into an equivalent square plate. See Fig. 12. The difference in area, ΔA, is equated to a square plate and the edge length is added to the width of the trapezoidal plate. Accordingly, the area removed equals:

$$\Delta A = 2(0.5c \cdot 1) \tag{19}$$

The change in edge length, Δb equals

$$\Delta b = \sqrt{c} \tag{20}$$

Hence

$$b_2' = 1 + \sqrt{c} \tag{21}$$

δ_y is taken equal to the new value of b_2. Values of δ_x and δ_y for the cases $b_1/b_2 = 0.4$, $b_1/b_2 = 0.6$, $b_1/b_2 = 0.8$ and $b_1/b_2 = 1.0$ at the load condition $\sigma_1/\sigma_2 = 1$ are given in Table 3.

$$\sigma_{cr} = \mu\left(\sigma_{rel,x}\beta_x\eta_x\delta_x\lambda_x + \sigma_{rel,y}\beta_y\eta_y\delta_y\lambda_y\right) \tag{22}$$

3.1. Illustrative case for an evolutive plate

Determine the buckling load of a simply supported evolutive aluminium plate, which is 2.5 mm thick, length 600 mm and has widths $b_1 = 160$ mm and $b_2 = 400$ mm and with $\sigma_1/\sigma_2 = 0.8$.

$b_1/ b_2 = 0.4$;
$c = (b_2 - b_1) / 2b_2 = 0.3$;
$\alpha = 600/400 = 1.5$;
$I_y = bt^3/12 = 400 \times 2.5^3/12 = 520.83$ mm^4 and
$I_x = at^3/12 = 600 \times 2.5^3/12 = 781.25$ mm^4.

Therefore

$$\sigma_{rel,x} = \left(\frac{\pi^2}{bt}\right)\left(\frac{EI_y}{a^2}\right) = 0.9995 \text{ N/mm}^2$$

$$\sigma_{rel,y} = \left(\frac{\pi^2}{at}\right)\left(\frac{EI_x}{b^2}\right) = 2.2489 \text{ N/mm}^2$$

From Table 1, $\beta_x = \beta_y = 1.000$, for uniform loading, $\lambda_x = \lambda_y = 1.000$
From Table 2, $\eta_x = 2.453$ and $\eta_y = 3.679$.
From Table 3, $\delta_x = 2.5$ and $\delta_y = 1.548$, and from Table 4, $\mu = 1.04$.
Substituting all these values into Eq. 22 gives $\sigma_{cr} = 19.693$ N/mm^2.
From Eq. 6, $\sigma_{ref} = 2.471$ N/mm^2. Therefore, the buckling coefficient $k = 19.693/2.471 = 7.97$.

A set of buckling coefficients for an evolutive plate with $\sigma1/\sigma2 = 0.8$ and with different b_1/ b_2 ratios is presented in Fig. 13 where comparisons are given with the design procedure and the results found from the HSB design code [16]. Other curves are found in Ahmed [14].
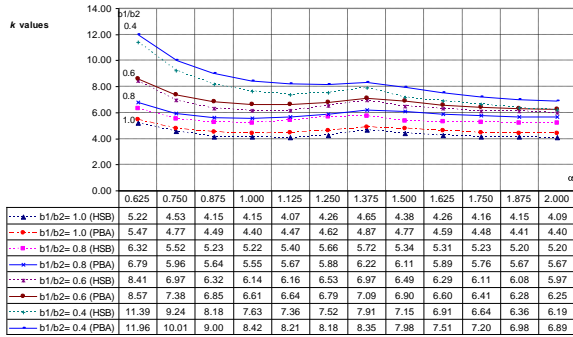

k values	b1/b2											α
	0.625	0.750	0.875	1.000	1.125	1.250	1.375	1.500	1.625	1.750	1.875	2.000
▲ b1/b2= 1.0 (HSB)	5.22	4.53	4.15	4.15	4.07	4.26	4.65	4.38	4.26	4.16	4.15	4.09
◇ b1/b2= 1.0 (PBA)	5.47	4.77	4.49	4.40	4.47	4.62	4.87	4.77	4.59	4.48	4.41	4.40
■ b1/b2= 0.8 (HSB)	6.32	5.52	5.23	5.22	5.40	5.66	5.72	5.34	5.31	5.23	5.20	5.20
✕ b1/b2= 0.8 (PBA)	6.79	5.96	5.64	5.55	5.67	5.88	6.22	6.11	5.89	5.76	5.67	5.67
✳ b1/b2= 0.6 (HSB)	8.41	6.97	6.32	6.14	6.16	6.53	6.97	6.49	6.29	6.11	6.08	5.97
● b1/b2= 0.6 (PBA)	8.57	7.38	6.85	6.61	6.64	6.79	7.09	6.90	6.60	6.41	6.28	6.25
✛ b1/b2= 0.4 (HSB)	11.39	9.24	8.18	7.63	7.36	7.52	7.91	7.15	6.91	6.64	6.36	6.19
━ b1/b2= 0.4 (PBA)	11.96	10.01	9.00	8.42	8.21	8.18	8.35	7.98	7.51	7.20	6.98	6.89

Fig. 13 Comparison of buckling values of a simply-supported evolutive plate with different b_1/b_2 ratios for $\sigma_1/\sigma_2 = 0.8$

4. Triangular Plates

To determine the critical buckling stress for a triangular plate subjected to normal uniform stress σ on all edges, the geometry of a triangular plate will be related to the geometry of a rectangular plate, as has been done for evolutive plates. The analysis assumptions considered in Section 2 are not completely applicable in this section because b_1 equals zero and consequently $1/b_1 \rightarrow \infty$. The plate shown in Fig.14 is related to a square plate with length a and width $b = a$. Let the modification parameter, as before, be δ and its components in the x and y directions be δ_x and δ_y, respectively.
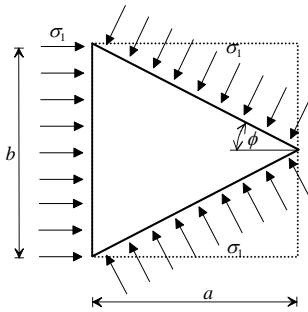

Fig. 14 Triangular plate and the equivalent rectangular plate

In the longitudinal i.e. x direction, the plate length a is constant, whilst the plate aspect ratio a increases with increasing α, i.e., the buckling coefficient k decreases. The parameter δ_x has to increase since the lateral edges move closer and stiffen the plate. The parameter δ_x is therefore related directly to the area of the rectangular plate and the triangular plates, and is given in Eq. 23.

$$\delta_x = \frac{Area\ rectangular\ plate}{Area\ triangular\ plate} = \frac{a \times b}{0.5 \times a \times b} = 2.0 \tag{23}$$

The parameter δ_y in the lateral direction has to decrease due to the additional stress $\Delta\sigma$ arising in the lateral y direction.

From Fig. 12, $\phi = tan^{-1}(b/2a)$ and the value of $\Delta\sigma_y$ is calculated by Eq. 24.

$$\Delta\sigma_y = \sigma_1 \cos\phi \tag{24}$$

The parameter δ_y in the lateral y direction is related to the stress component in the y direction $\Delta\sigma_y$ and is given in Eq. 25.

$$\delta_y = \cos\phi \tag{25}$$

The general equation for a triangular plate is shown in Eq. 26 (note that the stress ratio $\mu = 1.0$ in this case).

$$\sigma_{cr} = \sigma_{rel,x}\beta_x\eta_x\delta_x\lambda_x + \sigma_{rel,y}\beta_y\eta_y\delta_y\lambda_y \tag{26}$$

To check the equilibrium of the applied loads, the inclined lateral length a' is given in Eq. 27.

$$a' = \frac{a}{\cos\phi} \tag{27}$$

The applied lateral stress has two components, one in the x direction, σ_x, and one in the y direction, σ_y. The x component of the applied lateral stress is given in Eq. 28:

$$\sigma_x = \sigma_1 \sin\phi \tag{28}$$

The resultant, R of the stress determined in Eq. 29 is:

$$R = 2a'\sigma_1 \sin\phi = b\sigma_1 \tag{29}$$

The resultant R determined by Eq. 29 equals the resultant of the applied axial stress, or in other words, the plate is in equilibrium under the applied axial and lateral stresses.

4.1. Example to determine the buckling load of a triangular plate

Determine the buckling load of simply-supported, aluminium triangular plate, length 120 mm, width 160 mm, thickness 1.5 mm subjected to a uniform stress on all three sides. As before the aspect ratio and second moments of area α, I_x and I_y are 0.75, 45.00 mm^4 and 33.75 mm^4, respectively. The relative stresses $\sigma_{rel,x}$ and $\sigma_{rel,y}$ are obtained as 8.9957 N/mm^2 and 5.0601 N/mm^2 respectively from Eq. 2 and Eq. 3.
From Table 1, $\beta_x = \beta_y = 1.000$; for uniform loading, $\lambda_x = \lambda_y = 1.000$.
From Table 2, $\eta_x = 1.887$ and $\eta_y = 1.415$.
From Eq. 23 and Eq. 25, $\delta_x = 2.00$ and $\delta_y = 0.83$. Finally, applying Eq. 26, σ_{cr} is 39.91 N/mm^2.
Also from Eq. 6, σ_{ref} is 5.561 N/mm^2 and the corresponding buckling loading factor, k, is 39.91/5.561 = 7.18. This compares with the value found from finite element calculations of 6.70, about 7.1% different.
Fig. 15 shows a comparison of the buckling loads computed with the new design procedure against finite element [15] and the HSB [16] provisions.
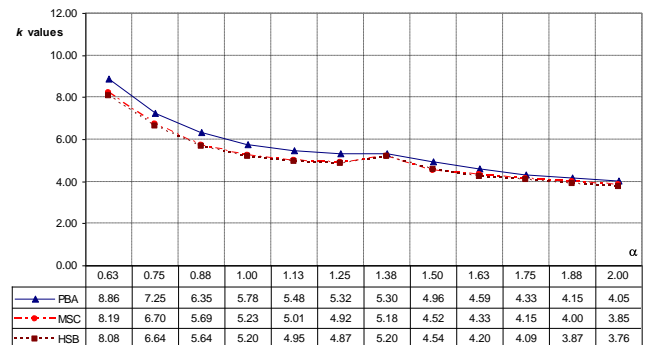

k values												α
	0.63	0.75	0.88	1.00	1.13	1.25	1.38	1.50	1.63	1.75	1.88	2.00
▲ PBA	8.86	7.25	6.35	5.78	5.48	5.32	5.30	4.96	4.59	4.33	4.15	4.05
● MSC	8.19	6.70	5.69	5.23	5.01	4.92	5.18	4.52	4.33	4.15	4.00	3.85
■ HSB	8.08	6.64	5.64	5.20	4.95	4.87	5.20	4.54	4.20	4.09	3.87	3.76

Fig. 15 Buckling coefficients for a triangular plate

5. Shallow cylindrical plates

In the previous section calculations of the critical buckling stresses were considered for flat plates. To extend the method to include shallow cylindrical plates (see Fig. 16) the moment of inertia I_y included in the plate relative buckling stress $\sigma_{rel,y}$ has to be modified for a curved plate, i.e., the displacement of the plate centre of gravity is to be included in the plate's second moment of area.
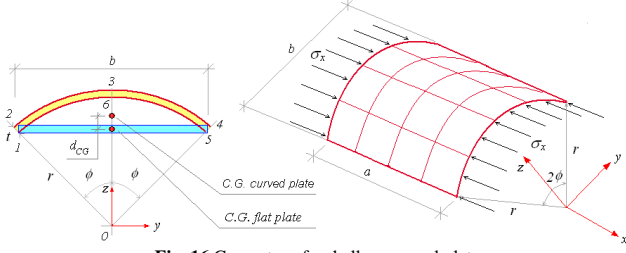
Fig. 16 Geometry of a shallow curved plate

The centre of gravity of a shallow cylindrically curved plate is displaced by an offset distance, d_{CG}, from the centre of gravity of a flat plate. The moment of inertia, I_y, is calculated as for beams with rectangular cross section as given in Eq. 30.

$$I_y = \frac{bt^3}{12} + bt\left(d_{cg}\right)^2 \tag{30}$$

To calculate the distance, d_{CG}, two virtual circle sectors are constructed. Fig. 16 shows the two circle sectors denoted by the corner points *0234* and *0165*. The sector *0234* has the centre of gravity at distance d_1 measured from point *0* in the *z* direction and the sector has area A_1. The sector *0165* has the centre of gravity at distance d_2 measured from point *0* in the *z* direction and the sector has area A_2. The distance d_{CG} given in Eq. 31 is determined by using Eqs. 32 to 35 [19].

$$d_{cg} = \left(r\cos\phi + \frac{t}{2}\right) - \left(\frac{d_1 A_1 - d_2 A_2}{A_1 - A_2}\right) \tag{31}$$

where:

$$d_1 = \frac{2(r+t)\sin\phi}{2\phi} \tag{32}$$

$$d_2 = \frac{2r\sin\phi}{3\phi} \tag{33}$$

$$A_1 = \frac{2\pi(r+t)^2\phi}{3\phi} \tag{34}$$

$$A_2 = \frac{2\pi r^2\phi}{360} \tag{35}$$

and ϕ is measured in degrees. Comparing the results of the modification with results of other methods such as the one described in HSB Design manual (16), the results are correct as long as d_{cg} is less than the plate thickness; otherwise for d_{cg} greater than the plate thickness, then the results are higher than reality. This is because the value of the term btd_{CG}^2 is greater than the term $bt^3/12$.

In the HSB Design manual [16], there is a limitation for the method based on research summarised by Gerard and Becker [20, 21]. The procedure s applicable if the condition given in Eq. 36 is valid.

$$\frac{100t}{r} \leq 1 \tag{36}$$

The allowable stress for the curved plate equals the allowable stress of the flat plate increased by a value $\Delta\sigma_{cr}$, and $\Delta\sigma_{cr}$ is calculated by Eq. 37.

$$\Delta\sigma_{cr} = 0.2E\left(\frac{t}{r}\right) \tag{37}$$

Consequently, for the new procedure there is also limitation to avoid error due to the term btd_{CG}^2. Therefore, if the increase in the critical buckling stress calculated using the term btd_{CG}^2 is higher than the value given by Eq. 37, then Eq. 37 must be used.

As an example, determine the buckling load of a simply-supported, aluminium, cylindrical plate, radius of curvature, 10000.0 mm, thickness 4.0 mm, width 200.0 mm, length 200.0 mm subjected to axial compression.

In this case the limitation condition of Eq. 36 is satisfied for all aspect ratios for which the method is applicable (i.e. $\alpha \leqslant 2$). The half sector angle $\phi = 100/10000$ rad = 0.773°.

Applying Eqs. 32 – 35, $d_1 = 6668.89$ mm, $d_2 = 6666.22$ mm, $A_1 = 2001733.78$ mm², $A_2 = 20001333.36$ mm² and $d_{cg} = 1.333$ mm.

According to Eq. 32 the moment of inertia of the flat plate about the *y* axis

is $I_y = 1066.67$ mm²; increment $\Delta I_y = 1422.49$ mm² and $I_x = 1066.67$ mm².

Using Eq. 1:

The plate relative stress in axial direction with ΔI_y is $\sigma_{rel,x} = 53.74$ N/mm², the plate relative stress in the lateral direction, $\sigma_{rel,y} = 23.03$ N/mm², the plate geometry terms $\sigma_{rel,x} = 53.74$ N/mm², $\eta_x = 2.198$ and $\eta_y = 2.198$, the critical buckling stress with ΔI_y, $\sigma_{cr} = 174.32$ N/mm², the critical buckling stress without ΔI_y, $\sigma_{cr} = 101.228$ N/mm².

The increase of the critical buckling stress due to the curvature of the plate determined using the design method equals $\Delta\sigma_{cr} = 174.32 - 101.28 = 73.04$ N/mm².

The increase of the critical buckling stress due to the curvature of the plate determined using the HSB design procedure (Eq. 37 equals $\Delta\sigma_{cr} = 174.32$ N/mm²). Hence, the value determined using the HSB procedure is selected.

Hence $\sigma_{ref} = 174.32$ N/mm² is given by

$$\sigma_{ref} = \frac{\pi^2 E}{12(1-v^2)}\left(\frac{t}{b}\right)^2 = 25.30 \tag{38}$$

The revised buckling load factor is therefore given by Eq. 39.

$$k = \frac{101.28 + 5.60}{25.30} = 4.22 \tag{39}$$

The results for all plates from the three methods, the new design procedure method, the classical method [16], and the FEM eigenvalue method [18], are put together in Fig.17.
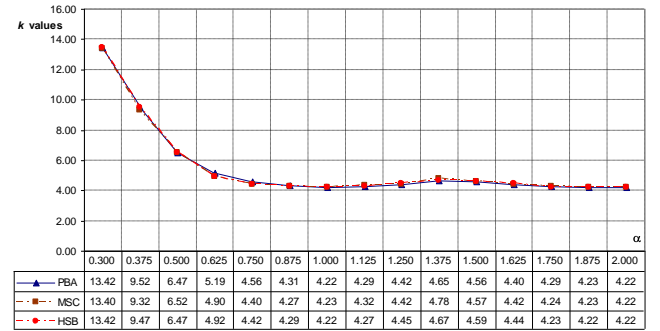

Fig. 17 Buckling coefficients for a simply-supported curved plates

6. Validation

To ensure that the calculations are correct two different methods were used to validate the results; namely by undertaking an eigenvalue analysis or by using a classical theoretical analysis method.

To determine the plate buckling stresses, the MSC/NASTRAN FEM software [15] with the CQUAD4 element and the DLUBAL/RSTAB FEM software [18] with the MITC4 shell element were used. Both elements have 6 degrees of freedom at each node (3 displacement and three rotational) was used to undertake a Mindlin/Reissner analysis [22]. The MSC/NASTRAN was able to analyse all possible plate geometries, i.e., rectangular, non-rectangular, and curved plates. DLUBAL/RSTAB , however, was only able to analyse rectangular flat plates.

To determine the plate buckling stresses based on the classical theoretical method, the literature presented by Bulson [6] and the HSB design manual [16, 17] were used.

A convergence analysis was carried out on different models with different mesh densities. A square plate simply supported on all edges was used to study the convergence of the analysis results. The plate width was 200 mm and the plate thickness was 10 mm. The loaded edge had a uniformly distributed axial stress of 0.05 N/mm² applied to it. To investigate convergence the plate was analysed using 4,16, 20, 80, 400 and 1280 elements. Results of the analyses using MSC/NASTRAN are collected in Table 5 and results from the analyses using DLUBAL/RSTAB are shown in Table 6.

Analysis showed that the results provided by the model with 400 elements were only marginally different from the results of the model with 1280 mesh elements. However, the analysis was carried out using elements with a length of 10 mm. All other plates using a similar mesh spacing.

Table 5
Results of the convergence analyses using MSC/NASTRAN

No. of Elements	4	16	20	80	400	1280
Critical buckling stress, σ_{cr}	784.7	670.5	670.7	642.3	634.0	633.0
Reference stress, σ_{ref}	158.2	158.2	158.2	158.2	158.2	158.2
Buckling coefficient, k	4.961	4.239	4.241	4.061	4.008	4.002

Table 6
Results of the convergence analyses using DLUBAL/RSTAB

No. of Elements	4	16	20	80	400	1280
Critical buckling stress, σ_{cr}	639.2	637.2	636.3	642.3	634.2	633.0
Reference stress, σ_{ref}	158.2	158.2	158.2	158.2	158.2	158.2
Buckling coefficient, k	4.041	4.029	4.023	4.017	4.010	4.008

Figs. 8-10,13, 17 7-9, 12, 15, 17 above show the results using the new design procedure and the corresponding curves using the finite element analyses or the exact theoretical results from the reference texts [6, 15-17].

During the validation process seven errors were investigated and their influence recorded. The errors were load offset (there is a small offset between the centre of gravity of a triangular load and that of a uniform load), deviation in the estimation of the load parameter λ (trapezoidal, biaxial and triangular loads are not exactly modelled in the derivation of λ), estimation of σ_{cr} for uniform stress (trapezoidal, biaxial and triangular loads are not exactly modelled in the derivation of σ_{cr}), estimation of the plate edge parameter β, (the curves developed by the approximations for β_x and β_y do not precisely follow the theoretical curves), estimation of the parameter η (determination of η is based on curve for plate configuration 01 which is not identical for those for cases 02to 18), the number of buckling waves (for plates under uniform stress with aspect ratios 0.3 and 2.0 where more than two waves can occur as the assumption only allow for 2 waves) and a basic assumption that the overall procedure does not work (this occurs when combinations of plate configurations 05 and 07).

In general, the errors produce an overall discrepancy between the design load and the finite element derivation of less than 4% which is suitable for preliminary design purposes. A full description of each derived curve and its errors is given in the Ahmed's thesis [14]. Slightly larger errors of the order of 10% occurred for free edge boundary conditions.

7. Conclusions

The new design procedure presented in [13, 14] by the authors has been extended to cover evolutive, triangular and cylindrical plates. The general procedure for the implementation of the method has been presented. The method has been validated against FEA and Code book predictions. The procedure is capable of determining buckling loads with very high accuracy of the order of 4% in most cases and about 10% different from FEA and design standards in the worst cases. The method can be implemented is a spreadsheet which makes its application to be faster than FEA methods. The method is particularly useful during design pre-sizing stages.

References

[1] Bryan G.H. "On the stability of a plane plate under thrusts in its own plane, with applications to the Buckling of the Sides of a Ship", Proceedings of the London Mathematical Society, 22, 54-67, 1890.
[2] Timoshenko S. and Gere J. "Theory of elastic stability", McGraw-Hill, 1961.
[3] Bleich F., "Buckling strength of metal structures", McGraw-Hill, 1952.
[4] Gerard G. and Becker H., "Handbook of structural stability, Part 1 – buckling of flat plates", N.A.C.A. Technical Note 3781, US, 1957.
[5] Gerard G., "Introduction to structural stability theory", McGraw Hill, 1962.
[6] Bulson P.S., "The stability of flat plates", Chatto and Windus Ltd., 1962.
[7] Dayyani I., Moore M. and Shahidi A., "Unilateral buckling of point-restrained triangular plates", Thin-Walled Structures, 66, 1-8, 2013.
[8] Tran K.L., Douthe C., Sab K., Dallot J. and Davaine L., "Buckling of stiffened curved panels under axial compression", Journal of Constructional Steel Research, 103, 140-147, 2014.
[9] Martins J.P., Simões da Silva L. and Silvetre N., "Energy-based analytical model to predict the elastic buckling of curved panels", Journal of Constructional Steel Research, 127, 165-175, 2016.
[10] Kim J-H., Park J-S., Lee K-H., Kim J-H., Kim M-H. and Lee K-M., "Computational analysis and design formula development for the design of curved plates for ships and offshore structures", Structural Engineering and Mechanics, 49, 6, 705-726, 2014.
[11] Bradford M.A. and Roufegarinejad A., "Unilateral and bilateral local buckling of thin-walled plates with Built-in Edges", Proceedings of the Fifth International Conference on Thin-walled Structures, Brisbane, 15- 28, 2008.
[12] Liew K.M. and Wang C.M., "Elastic buckling of regular polygonal plates", Thin-Walled Structures, 21, 163-173, 1995.
[13] Ahmed H., Durodola J. and Beale R.G., "A new design approach for the determination of the buckling load of rectangular plates", Proc. Inst. Mech Eng., Part C, J. Mech. Eng. Sci., 227, Issue July, 1417-1428, 2013.
[14] Ahmed H., "A new parametric buckling analysis approach for plates", PhD Thesis, Oxford Brookes University, Oxford, UK, 2013.
[15] MSC Nastran. http://www.mscsoftware.com, accessed 21:02:2011.
[16] HSB, "Handbuch Struktur Berechnung", Prepared by L. Schwarmann and J. Ribke, LTH committee, Germany, part 45, 1975.
[17] HSB, http://www.fatec-engineering.com/2017/02/17/hsb-structural-analysis-manual/, Accessed 19:03:2017.
[18] RSTAB 7.xx, "Dlubal Ing. Software", http://www.ng.dlubal.com, accessed 21:02:2011.
[19] Murray, S. and Liu, J., "Schaums mathematical handbook of formulas and tables", McGraw-Hill, 2003.
[20] Gerard G. and Becker H., "Handbook of structural stability part 1 – buckling of flat plates", NACA TN 3781, 1957.
[21] Gerard G. and Becker H., "Handbook of structural stability part 3 – buckling of curved plates and shells", NACA TN 3783, 1957.
[22] Mindlin R.D., "Influence of rotatory inertia and shear on flexural motions of isotropic, elastic plates," ASME Journal of Applied Mechanics, 18, 31–38, 1951.